

Saturation of THz-radiation power from femtosecond-laser-irradiated InAs in a high magnetic field

Hideyuki Ohtake,^{a)} Shingo Ono,^{b)} Masahiro Sakai, Zhenlin Liu, Takeyo Tsukamoto,^{b)} and Nobuhiko Sarukura^{c)}

Institute for Molecular Science (IMS), Myodaiji, Okazaki 444-8585, Japan

(Received 13 December 1999; accepted for publication 19 January 2000)

THz-radiation power from femtosecond-pulse-irradiated InAs is found to be saturated at the magnetic field around 3 T. Additionally, we find that this saturation magnetic field strongly depends on geometrical layout. Interesting magnetic-field dependence of the center frequency for THz radiation is also observed. © 2000 American Institute of Physics. [S0003-6951(00)03311-8]

There have been numerous necessities for intense, compact, and simple THz-radiation sources,¹⁻⁷ which can be applied for sensing, imaging, and time-resolved spectroscopy.⁸⁻¹⁰ Zhang *et al.* reported enhancement of THz-radiation power due to quadratic magnetic-field dependence of THz-radiation power (up to 0.3 T) from GaAs irradiated with a femtosecond laser.¹¹ Previously, we also reported the significant enhancement of THz-radiation power from InAs in a magnetic field irradiated with femtosecond optical pulses, owing to quadratic magnetic-field and quadratic excitation intensity dependence of THz-radiation power.^{12,13} From the practical point of view, the advantage of using InAs as a THz emitter is approximately one order higher efficiency of THz-radiation power compared with the GaAs case due to its smaller effective mass.¹² To design useful THz-radiation sources, it is strongly required to examine the scalability of THz-radiation power with this magnetic-field enhancement scheme. In this letter, we report saturation of THz-radiation power from femtosecond-laser-irradiated InAs in a high magnetic field and magnetic-field dependence of THz-radiation spectra. We also present magnetic-field direction dependence of THz-radiation power and spectra.

The experimental setup is almost similar to that of Ref. 12. An 82 MHz repetition-rate mode-locked Ti:sapphire laser delivers nearly transform-limited 70 fs pulses at 800 nm. The sample is undoped bulk InAs with a (100) surface. The average power for excitation is about 700 mW with 3 mm spot size in diameter on the sample. A split-coil superconducting magnet with cross-room-temperature bores can provide a magnetic field up to 5 T. With this specially designed magnet, five different optical geometries, as illustrated in Fig. 1, are compared by changing the magnetic field, magnetic-field direction, and excitation laser incident angle. A liquid-helium-cooled silicon bolometer is provided for detecting the power of the total radiation and a wire-grid polarizer is placed in front of the bolometer as shown in the insets of Fig. 2. The THz radiation polarizes almost horizontally, as shown in Fig. 2(a). From lower magnetic field to

near 2 T, the THz-radiation power shows quadratic magnetic-field dependence.¹² Moreover, in the case of the magnetic field parallel to the surface and the laser incident angle 45° to the surface normal (G-1), the saturation at around 3 T and the reduction of the radiation power above 3 T are observed. On the contrary, clear saturation is not observed in the case of the G-5 (G-5: the magnetic field parallel to the THz-radiation propagation direction and the laser incident angle 45° to the surface normal), as shown in Fig. 2(b). In the case of the G-5 geometrical layout, the polariza-

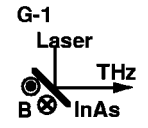
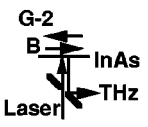
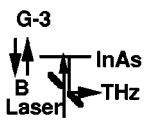
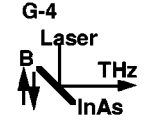
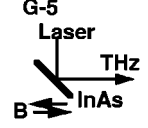
Geometry	Magnetic field direction	Saturation field (T)	Relative power
G-1 	⊗ ⊙	+3.2 -3.0	1 (max) 0.77
G-2 	N → S S ← N	+3.2 -3.1	0.11 0.10
G-3 	No radiation was observed.		
G-4 	S ↑ N ↓ N ↓ S ↑	+4.8 -4.7	0.67 0.67
G-5 	N → S S ← N	+5.0 > -5.0 >	0.70 0.68

FIG. 1. Geometry dependence of THz-radiation power. The saturation of THz-radiation power is observed in the upper two cases. The magnetic field is parallel to the (011) crystal axis in the G-1, G-2 geometrical layouts, and the (100) axis in the G-3 geometrical layout, respectively. In the case of the G-4 and G-5 geometrical layouts, the magnetic field is 45° to the surface normal.

^{a)}Electronic mail: ohtake@ims.ac.jp

^{b)}Science University of Tokyo, Kagurazaka 1-3, Shinjuku, 162-8601, Japan.

^{c)}Also at: Kanagawa Academy of Science and Technology, Takatsu-ku, Kawasaki 213-0012, Japan.

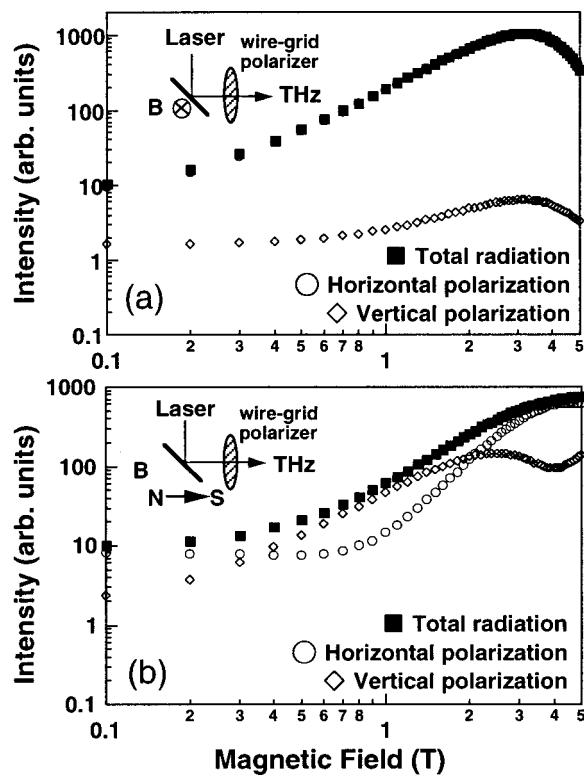


FIG. 2. Magnetic-field dependence of THz-radiation power. The inset indicates the experimental setup for the G-1 and the G-5 geometrical layouts. (a) for the G-1 and (b) for the G-5 geometrical layouts, respectively. Clear saturation is observed at around magnetic field 3 T in the case of the G-1 geometrical layout.

tion of the THz radiation changed dramatically with increasing magnetic field. Photoexcited electrons are accelerated on the plane that is perpendicular to the propagation direction of the THz radiation in the G-5 geometrical layout. Since the polarization of THz radiation reflects the projection of the carrier accelerating direction to each direction, both components of polarization should be observed. Figure 3 illustrates the time-domain measurement of the THz-radiation electric field from InAs in the G-1 geometrical layout with a 1-T permanent magnet. A dipole antenna is used as a receiver for THz radiation. There is a very clear difference between those two cases. In Fig. 3(a), the phase of the field oscillation is completely opposite, because the photoexcited electrons are accelerated to the opposite directions by the magnetic field. Thus, the spectral shapes in Fig. 3(b) show a clear difference. The five geometrical layouts are schematically illustrated in the first column of Fig. 1. The saturation of THz-radiation power is observed only in the G-1 and G-2 geometrical layouts (G-2: the magnetic field parallel to the THz-radiation propagation direction and the laser incident angle perpendicular to the surface). Additionally, in the G-1 geometrical layout, we have observed the remarkable magnetic-field direction dependence of the THz-radiation power. This result also originates from the difference of the electron acceleration direction. We are currently working to clarify the saturation mechanism with a combination of time-resolved spectroscopy and complicated magnetic direction dependence of THz-radiation power and spectra. One possible explanation for this saturation is as follows. Under this experimental condition, photoexcited electrons in the Γ valley may be scat-

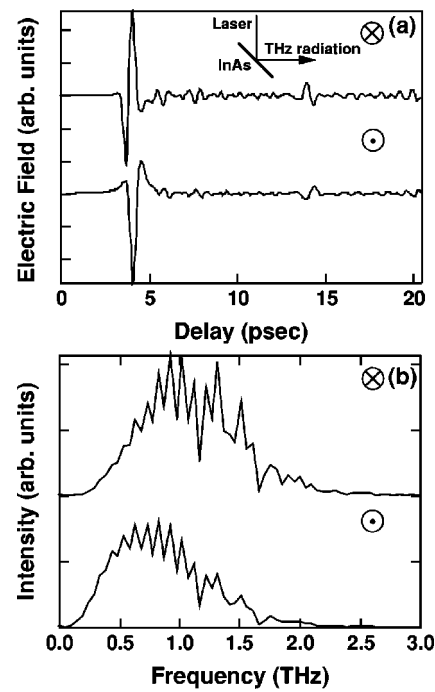


FIG. 3. Time-domain measurement for THz radiation. (a) Delay dependence of electric field from InAs in 1.0 T magnetic field. The direction of the magnetic field is described in the insets. The phases are completely different from each other. (b) THz-radiation spectra. The interference patterns are due to the dipole antenna, in which the substrate is transparent in the terahertz region.

tered to the L valley by Lorentz acceleration of electrons due to the magnetic field, as observed in the electric-field case.¹⁴ This process will reduce the number of electrons in the Γ valley contributing to generating THz radiation.

Detailed THz-radiation spectra have been also obtained by a polarizing Michelson interferometer. To extract the features of the THz-radiation spectra in various cases, the center frequency and the spectral width of the THz radiation is defined as the average and the standard deviation of the frequency between 0.05 and 5 THz by integration. Both the center frequency and the spectral width show interesting magnetic-field dependence that differs significantly with the optical layout, as shown in Fig. 4. In Figs. 4(b) and 4(c), for the G-5 geometrical layout, the center frequency shows sym-

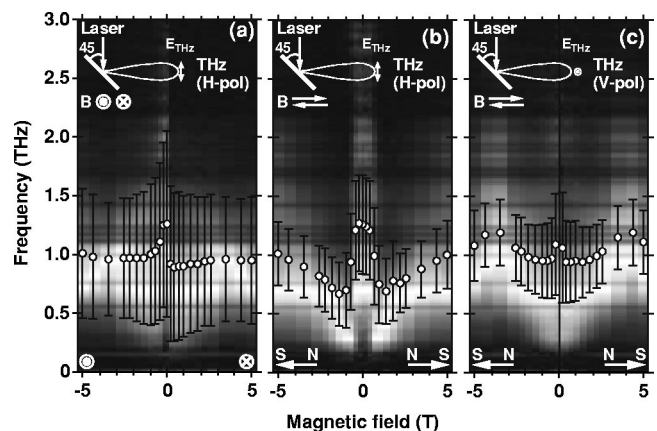


FIG. 4. Two-dimensional plots for THz-radiation spectra on different magnetic fields. (a) for the G-1, and (b) and (c) for the G-5 geometrical layouts. Open circles and bars show the center frequency and spectral bandwidth, respectively. H-pol and V-pol indicate horizontal and vertical polarization.

metric magnetic-field direction dependence, as expected from the motion of the electrons. On the other hand, asymmetric magnetic-field direction dependence of THz radiation is shown in Fig. 4(a) for the G-1 geometrical layout. The relative powers could be compared with all geometrical layouts. The maximum power is obtained in the case of the G-1 geometrical layout. As mentioned in the time-resolved measurement, the electrons are accelerated to the opposite directions with changing magnetic-field directions in the G-1 geometrical layout. Therefore, the center frequency should be changed. While in the case of the G-5 geometrical layout, since both the upward and the downward electron acceleration cause the same polarization of THz radiation, we can observe the same spectra even in the opposite magnetic field. This explanation is applied for the G-2 and G-4 geometrical layouts (G-4: the magnetic field and the laser incident angle are 45° to the surface normal).

In conclusion, we have found saturation of THz-radiation power in high magnetic field. The optimum magnetic field is 3 T, as shown in Fig. 1. We have also observed an interesting dependence of the frequency and spectral width of the radiation. From the practical point of view, to design compact and intense THz-radiation sources, the optimum magnetic field is found to be around 3 T from these experiments. This magnetic field will be easily achieved by our permanent magnet.¹⁵ Additionally, the geometry-dependent saturation behavior and spectral shift should imply very rich physics of semiconductors to be explored.

The authors would like to express their gratitude to Professor K. Sakai and Dr. M. Tani in the Communications Research Laboratory for their collaboration work and discussion. The authors are thankful to E. Kawahata for his helpful assistance in the experiment. This research was partially sup-

ported by a Grant-in-Aid for Scientific Research on Priority Areas (11231204) and Grant-In-Aid for Encouragement of Young Scientists (10750038) from The Ministry of Education, Science, Sports and Culture, NEDO Japan Small and Medium Enterprise Cororation, Creative and Fundamental R&D Program for SMEs, "Research for the Future (RFTF)" of Japan Society for the Promotion of Science (JSPS-RFTF 99P01201), the Research Foundation for Opto-Science and Technology, and a Sasakawa Scientific Research Grant from The Japan Science Society.

- ¹D. H. Auston, *Appl. Phys. Lett.* **43**, 713 (1983).
- ²D. Krokkel, D. Grischkowsky, and M. B. Ketchen, *Appl. Phys. Lett.* **54**, 1046 (1989).
- ³P. C. M. Planken, M. C. Nuss, W. H. Knox, D. A. B. Miller, and K. W. Goossen, *Appl. Phys. Lett.* **61**, 2009 (1992).
- ⁴I. Brener, D. Dykaar, A. Frommer, L. N. Pfeiffer, J. Lopata, J. Wynn, K. West, and M. C. Nuss, *Opt. Lett.* **21**, 1924 (1996).
- ⁵M. Hangyo, S. Torazawa, Y. Murakami, M. Tonouchi, M. Tani, Z. Wang, K. Sakai, and S. Nakashima, *Appl. Phys. Lett.* **69**, 2122 (1996).
- ⁶K. A. McIntosh, E. R. Brown, K. B. Nichols, O. B. McMahon, K. M. Molvar, W. F. DiNatale, and T. M. Lyszczarz, *Appl. Phys. Lett.* **67**, 3844 (1995).
- ⁷K. Kawase, M. Sato, and H. Itoh, *Appl. Phys. Lett.* **68**, 559 (1995).
- ⁸D. M. Mittleman, S. Hunsche, L. Boivin, and M. C. Nuss, *Opt. Lett.* **22**, 904 (1997).
- ⁹M. Exter, C. Fattinger, and D. Grischkowsky, *Opt. Lett.* **14**, 1128 (1989).
- ¹⁰B. I. Greene, J. F. Federici, D. R. Dykaar, A. F. J. Levi, and L. Pfeiffer, *Opt. Lett.* **16**, 48 (1991).
- ¹¹X.-C. Zhang, Y. Lin, T. D. Hewitt, T. Sangsiri, L. E. Kingsley, and M. Weiner, *Appl. Phys. Lett.* **62**, 2003 (1993).
- ¹²N. Sarukura, H. Ohtake, S. Izumida, and Z. Liu, *J. Appl. Phys.* **84**, 654 (1998).
- ¹³S. Izumida, S. Ono, Z. Liu, H. Ohtake, and N. Sarukura, *Appl. Phys. Lett.* **75**, 451 (1999).
- ¹⁴For example, D. M. Caughey and R. E. Thomas, *Proc. IEEE* **55**, 2192 (1967); S. M. Sze, *Physics of Semiconductor Devices*, 2nd ed. (Wiley, New York, 1981).
- ¹⁵S. Ono, T. Tsukamoto, M. Sakai, Z. Liu, H. Ohtake, N. Sarukura, S. Nishizawa, and A. Nakanishi in *Rev. Sci. Instrum.* **71**, 554 (2000).